Different Complexation Behavior of Fe(III), Co(II) and Ni(II) with Pyridine-2,6-dicarboxylic Acid and 4,4´-Bipyridine Adduct: Syntheses, Crystal Structures and Solution Studies

J. Soleimannejad[a,*], H. Aghabozorg[b], Y. Mohammadzadeh[a], M. Nasibipour[a], S. Sheshmani[c], A. Shokrollahi[d], E. Karami[d] and M. Shamsipur[e]

[a]*Department of Chemistry, Ilam University, Ilam, Iran*
[b]*Faculty of Chemistry, Tarbiat Moallem University, Tehran, Iran*
[c]*Department of Chemistry, Islamic Azad University, Shahr-e Rey Branch, Tehran, Iran*
[d]*Department of Chemistry, Yasouj University, Yasouj, Iran*
[e]*Department of Chemistry, Razi University, Kermanshah, Iran*

Three complexes (bpyH)[Fe(pydc)$_2$].4H$_2$O (**1**), [Co$_2$(pydc)$_2$(μ-bpy)(H$_2$O)$_4$].4H$_2$O (**2**) and [Ni(pydc)(bpy)(μ-bpy)]$_4$.8H$_2$O (**3**) were prepared from the reaction between pyridine-2,6-dicarboxylic acid, pydcH$_2$, and 4,4´-bipyridine, bpy, with FeCl$_2$.4H$_2$O, CoCl$_2$.6H$_2$O and NiSO$_4$.6H$_2$O, respectively. The complex (**1**) crystallizes in the space group $P\bar{1}$ of the triclinic system and contains two molecules per unit cell. The structure has been refined to a final value for R factor of 0.0355 based on 4922 reflections. The crystal structure shows that Fe(III) is coordinated to two pyridine-2,6-dicarboxylate ligands. The complexes (**2**) and (**3**) crystallize in the space group $P2_1/c$ of the monoclinic system and contain two molecules per unit cell. The structure (**2**) has been refined to a final value for R factor of 0.0295 based on 2249 reflections. The molecular structure (**2**), which is a binuclear complex, contains two pyridine-2,6-dicarboxylate ligands, and a 4,4´-bipyridine bridge ligand. The structure (**3**) has been refined to a final value for R factor of 0.0579 based on 7721 reflections. In this structure, which is a tetramer complex, pyridine-2,6-dicarboxylate and 4,4´-bipyridine fragments act as a tri- and bidentate ligands, respectively. The protonation constants of 4,4´-bipyridine and pyridine-2,6-dicarboxylate, the equilibrium constants for the pydc-bpy system and the stoichiometry, and stability of complexation of this system with Fe^{3+}, Co^{2+} and Ni^{2+} ions in a aqueous solution were investigated by potentiometric pH titration method. The stoichiometry of the most complexes species in solution was found to be very similar to the crystalline cited metal ion complexes.

Keywords: Pyridine-2,6-dicarboxylic acid, 4,4´-Bipyridine, Fe(III), Co(II) and Ni(II) complexes, Crystal structures, Non-covalent interactions, Solution studies

INTRODUCTION

Existing design strategies for the synthesis of

supramolecular systems and extended inorganic networks follow two principal methods based on the different nature of the interactions responsible for networking. In one approach, which is the more frequently used, coordinative covalent bonds engaged between transition-metal ions and various

*Corresponding author. E-mail: janet_soleimannejad@yahoo.com

organic linkers propagate the coordination geometry into infinite architectures of various dimensionality and topology [1-5]. The other method, still far less common, exploit weaker intermolecular forces (particularly π-π interactions, H-bonding, and ion-pairing) as a guide to the assembly of molecular coordination complexes into extended organized networks [2]. In both cases, seeking for new and alternative approaches for easily building organized inorganic supramolecular arrays is one of the main aims.

In recent years, our research group has studied and worked on the synthesis and characterization of supramolecular systems, and its complexation with different metal ions. We have found out the role of non-covalent interactions such as hydrogen bonding, ion pairing and π-π stacking in constructing the supramolecular crystalline compounds and their metal complexes [6-19]. We trace a type of crystal engineering, which is the design and preparation of a crystalline material based on a knowledge, or at least consideration, of the steric, topological and intermolecular bonding capabilities of the constituent building blocks specially by taking advantage of hydrogen bonding. In continuation of previous research works, in this paper different complexation behavior of Fe(III), Co(II) and Ni(II) with pyridine-2,6-dicarboxylic acid and 4,4´-bipyridine adduct is discussed.

EXPERIMENTAL

Chemicals and Apparatus

All chemical used were of commercial suppliers and used without any further purification. Doubly distilled deionized water was used in the procedures when needed.

Melting points were determined with Electrothermal IA-9100 and were not corrected. IR spectra were recorded on a Bomem MB-100 spectrophotometer using KBr discs or Nujol mulls. Elemental analysis was obtained from a Perkin Elmer 2400 analyzer. X-ray structure analysis of suitable single crystals were carried out on a Bruker-AXS SMART diffractometer with an APEX CCD area detector (Mo-Kα radiation, graphite monochromator, λ = 0.71073 Å). The data were corrected for polarization and Lorentz effects, and an empirical absorption correction (SADABS) was applied [20]. The structures were solved by SHELXS-97 [21]. The non-hydrogen atoms were refined anisotropically by the full matrix

least-square method based on F^2 using SHELXL-97 [21].

Potentiometric Equilibrium Measurements

A Model 794 Metrohm Basic Titrino was attached to an extension combined glass-calomel electrode mounted in an air-protected, sealed, thermostated jacketed cell maintained at 25.0 ± 0.1 °C by circulating water, from a constant-temperature bath Fisherbrand model FBH604, LAUDA, Germany, equipped with a stirrer and a 10.000-ml-capacity Metrohm piston burette. The *p*H meter-electrode system was calibrated to read -log[H⁺].

The details are described in previous publications [15,22-24]. The concentration of bpy and pydc was 2.50×10^{-3} M, for the potentiometric *p*H titrations of pydc, bpy and pydc-bpy system, in the absence and presence of 1.25×10^{-3} metal ions. A standard carbonate-free NaOH solution (0.0927 M) was used in all titrations. The ionic strength was adjusted to 0.1 M with KNO_3. Before an experimental point (*p*H) was measured, sufficient time was allowed for the establishment of equilibrium. Ligands' protonation constants and stability constants of adduct and their metal complexes were evaluated using the BEST program described by Martell and Motekaitis [25]. The value of $K_w = [H^+][OH^-]$ used in the calculations according our previous works [15,22,23].

Synthesis of (bpyH)[Fe(pydc)₂].4H₂O Complex, (1)

An aqueous solution of pyridine-2,6-dicarboxylic acid (312 mg, 2 mmol) and 4,4´-bipyridine (167 mg, 1 mmol) in water (15 ml) which was already refluxed for one hour, was added to a solution of $FeCl_2.4H_2O$ (99 mg, 0.5 mmol) in water (5 ml) and heated for a further one hour at 70 °C. Green crystals of the complex, suitable for X-ray analysis, were obtained by slow evaporation of the solution at room temperature after two weeks. The procedure adopted in the synthesis of complex (**1**) is outlined in Scheme 1. This complex was characterized by IR spectroscopy, CHN analysis and single crystal X-ray diffraction. m.p.: 269 °C, Yield: 76%. Anal. Calcd. for $C_{24}H_{23}FeN_4O_{12}$: C, 50.70; H, 4.10; N, 9.86; Found: C, 49.92; H, 4.20; N, 10.00.

Synthesis of [Co₂(pydc)₂(μ-bpy)(H₂O)₄].4H₂O Complex, (2)

To a solution of 4,4´-bipyridine (624 mg, 4 mmol) and pyridine-2,6-dicarboxylic acid (167 mg, 1 mmol) in water (15
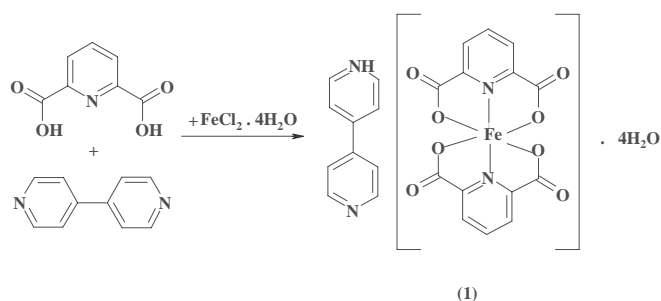
Scheme 1. The method for the synthesis of complex (**1**)

ml) that heated for one hour, was added a solution of $CoCl_2.6H_2O$ (238 mg, 1 mmol) in water (5 ml). This solution was heated at 90 °C for 3 h. Red crystals were obtained after one week by the slow evaporation of the solvent at room temperature. The procedure adopted in the synthesis of complex (**2**) is shown in Scheme 2. The characterization was carried out by IR spectroscopy, CHN analysis and single crystal X-ray diffraction. m.p.: >380 °C, Yield: 43%. Anal. Calcd. for $C_{24}H_{30}Co_2N_4O_{16}$: C, 38.54; H, 4.01; N, 7.49; Found: C, 38.87; H, 4.26; N, 7.82.

Synthesis of [Ni(pydc)(bpy)(μ-bpy)]₄.8H₂O Complex, (**3**)

To a solution of pyridine-2,6-dicarboxylic acid (167 mg, 1 mmol) and 4,4´-bipyridine (312 mg, 2 mmol) in water (10 ml) that heated for one hour, was added an aqueous solution of $NiSO_4.6H_2O$ (132 mg, 0.5 mmol) in water (5 ml). This mixture was heated at 60 °C for 30 min. Blue crystals were obtained after 10 days by the slow evaporation of the solvent at room temperature. The synthesis of the complex (**3**) is

shown in Scheme 3. This complex was characterized by IR spectroscopy, and single crystal X-ray diffraction. m.p.: 240 °C, Yield: 51%. Anal. Calcd. for $C_{108}H_{106}N_{20}Ni_4O_{31}$: C, 53.67; H, 4.39; N, 11.60; Found: C, 53.75; H, 4.42; N, 11.67.

RESULTS AND DISCUSSION

IR Studies of Complexes

The presence of 4,4´-bipyridine and pyridine-2,6-dicarboxylate in these complexes were confirmed by IR spectroscopy. The IR spectra contained several indicative peaks such as an absorption band at 1400-1600 cm^{-1} which refers to the stretching vibration of C=O bond, the stretching frequencies due to the aromatic rings at 3000-3100 cm^{-1} and a broad band at the region of 3000 cm^{-1} due to the N$^+$H groups. The lattice water frequencies appeared at the 3000-3400 cm^{-1} (anti-symmetric and symmetric OH stretching) and 1600-1630 cm^{-1} regions (HOH bendings).

X-ray Crystal Structure of (bpyH)[Fe(pydc)₂].4H₂O Complex, (**1**)

The molecular structure and the crystal packing diagram of complex (**1**) are illustrated in Figs. 1 and 2, respectively. The C-O···π and C-H···π interactions in this complex are shown in Fig. 3. Table 1 lists a summary of X-ray crystallographic data and Table 2 shows selected bond lengths, angles and torsion angles for this complex. A list of hydrogen bonds is also given in Table 3.

This complex crystallizes in the space group $P\bar{1}$ of the triclinic system and contains two molecules per unit cell. Important features of the crystal structure are complexation of two pyridine-2,6-dicarboxylates as tridentate ligands and
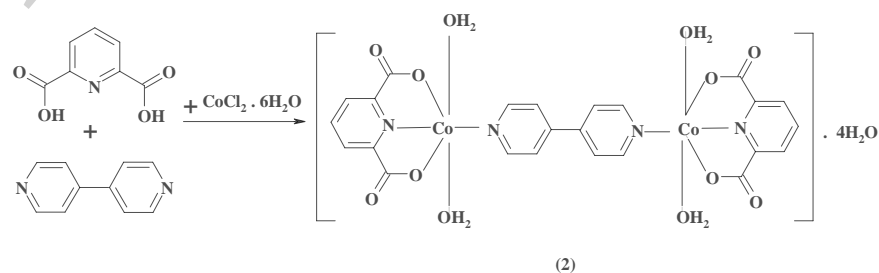
Scheme 2. The method for the synthesis of complex (**2**)

(3)
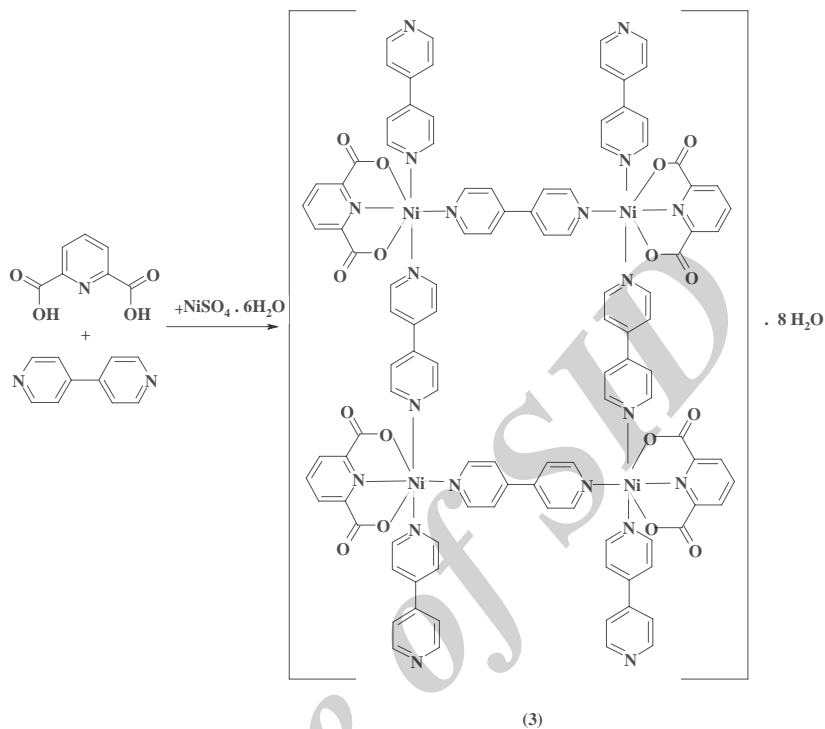
Scheme 3. The method for synthesis of complex (**3**)

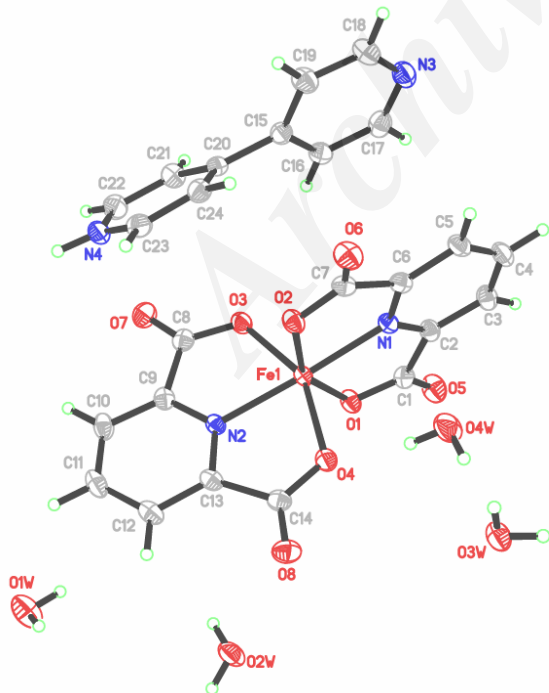**Fig. 1.** Molecular structure of complex (**1**).

formation of an anionic complex $[Fe(pydc)_2]^-$, and cationic counter ion $(bpyH)^+$. The Fe(III) is hexacoordinated by two nitrogen atoms N(1), and N(2) and four oxygen atoms O(1), O(2), O(3) and O(4) of carboxylate groups of two $(pydc)^{2-}$. Figure 1 and Table 2 show that the Fe(III) atom is located in the center of a distorted octahedral arrangement. The N(1)-Fe-N(2) angle shows deviation from linearity, 170.90(6)°. The O(2)-Fe(1)-O(3)-C(8), O(2)-Fe(1)-O(4)-C(14), O(4)-Fe(1)-O(1)-C(1) and O(4)-Fe(1)-O(2)-C(7) torsion angles are -93.74(13)°, 86.75(14)°, -102.35(14)° and 94.37(14)°, respectively, indicating that two dianionic $(pydc)^{2-}$ units are almost perpendicular to each other. Another characteristic solid state structural feature of this complex is dictated by the presence of 4,4′-bipyridinium fragment as a proton acceptor that deprotonates pyridine-2,6-dicarboxylic acid. This can lead to the formation of a metal-organo Fe(III) complex in which ion-pairing, metal-ligand coordination and hydrogen-bonding play important roles in the construction of its three dimensional supramolecular network.

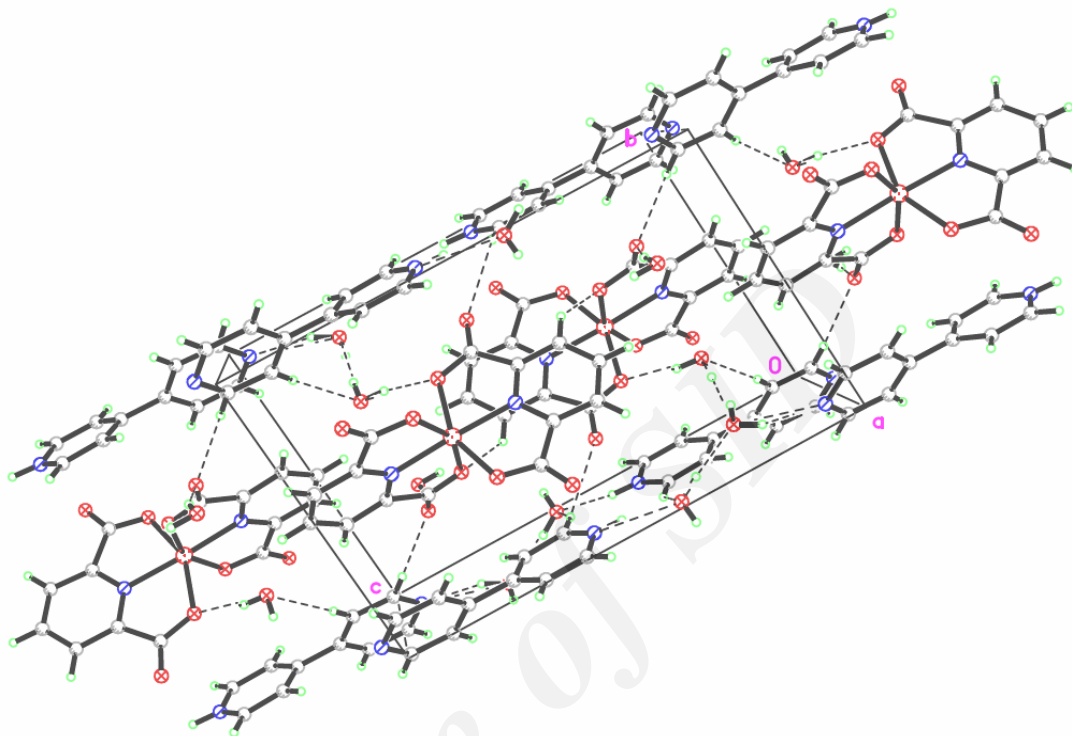It is of interest to note that the crystal packing diagram

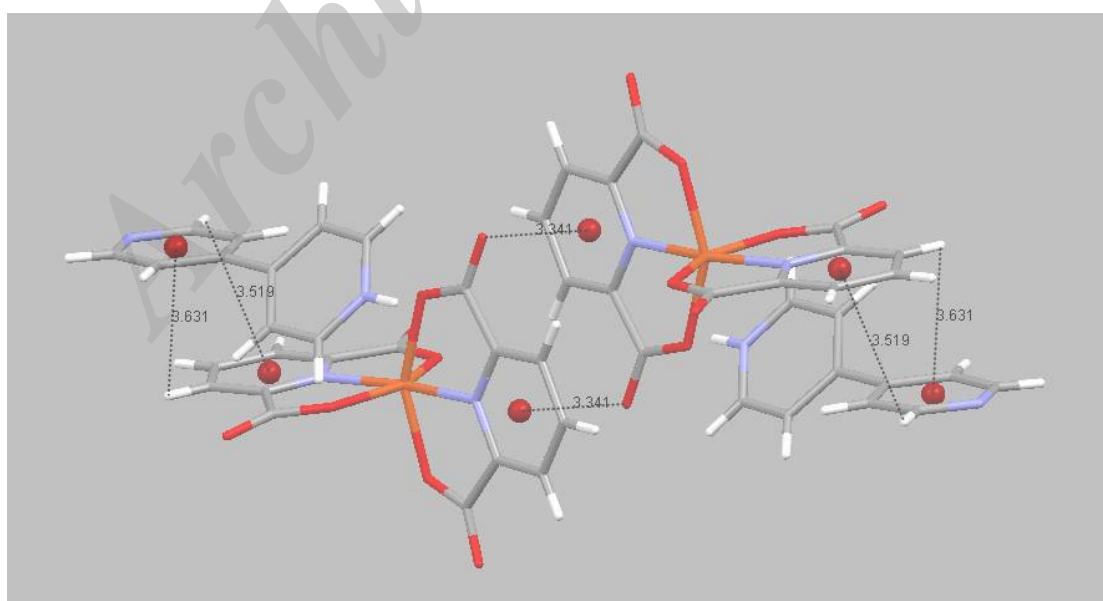**Fig. 2.** Crystal packing diagram of complex (**1**).

Fig. 3. The C-O···π and C-H···π interactions in complex (**1**).

251

Table 1. Crystallography Data for Complexes (**1**), (**2**) and (**3**)

	Complex (1)	Complex (2)	Complex (3)
Empirical formula	$C_{24}H_{23}FeN_4O_{12}$	$C_{24}H_{30}Co_2N_4O_{16}$	$C_{108}H_{106}N_{20}Ni_4O_{31}$
Formula weight	615.31	748.38	2414.97
Temperature (K)	150(2)	150(2)	150(2)
Wavelength	0.71073 Å	0.71073 Å	0.71073 Å
Crystal system	Triclinic	Monoclinic	Monoclinic
Space group	$P\bar{1}$ $Z = 2$	$P2_1/c$ $Z = 2$	$P2_1/c$ $Z = 2$
Unit cell dimensions	$a = 9.3759(9)$Å $\alpha = 84.545(2)°$	$a = 10.5154(8)$Å	$a = 20.631(7)$Å
	$b = 9.3778(9)$Å $\beta = 89.246(2)°$	$b = 20.1104(15)$Å $\beta = 107.844(5)°$	$b = 14.872(5)$Å $\beta = 115.854(6)°$
	$c = 14.6284(14)$Å $\gamma = 87.062(2)°$	$c = 7.3280(5)$Å	$c = 19.449(7)$Å
Unit cell volume	1278.7(2)Å^3	1475.10(19)Å^3	5370(3)Å^3
Calculated density (g cm^{-3})	1.598	1.685	1.494
Absorption coefficient	0.665 mm^{-1}	1.208 mm^{-1}	0.782 mm^{-1}
Crystal dimentions (mm^3)	$0.39 \times 0.39 \times 0.28$	$0.32 \times 0.21 \times 0.18$	$0.21 \times 0.18 \times 0.16$
F(000)	634	768	2508
θ range for data collection	2.47 to 28.64°	2.03 to 25.00°	2.18 to 26.09°
Limiting indices	$-12 \leq h \leq 11, -12 \leq k \leq 12, -19 \leq l \leq 19$	$-12 \leq h \leq 12, -23 \leq k \leq 23, -8 \leq l \leq 8$	$-26 \leq h \leq 26, -19 \leq k \leq 19, -26 \leq l \leq 25$
Reflections collected	14814	13265	15146
Completeness to θ	θ = 2.47 to 28.64°	θ = 2.28 to 30.43°	θ = 2.18 to 26.9°
Refinement method	Full-matrix least-squares on F^2	Full-matrix least-squares on F^2	Full-matrix least-squares on F^2
Goodness-of-fit on F^2	1.038	1.097	1.054
Final R indices [I > 2sigma(I)]	$R1 = 0.0355, wR2 = 0.0942$	$R1 = 0.0295, wR2 = 0.0788$	$R1 = 0.0579, wR2 = 0.1529$
R indices (all data)	$R1 = 0.0455, wR2 = 0.0987$	$R1 = 0.0371, wR2 = 0.0837$	$R1 = 0.1083, wR2 = 0.1734$
Largest diff. peak and hole	0.001 and 0.000 e. Å^{-3}	0.000 and 0.000 e. Å^{-3}	0.001 and 0.000 e. Å^{-3}

Crystallographic data for the three structures have been deposited with the Cambridge Crystallographic Data Centre, CCDC 767012 for the Fe(II) complex, CCDC 767011 for the Co(II) complex and CCDC 767010 for Ni(II) complex. Copies of the data can be obtained free of charge on application to the Director, CCDC, 12 Union Road, Cambridge CB2 1EZ, UK (Fax: int.code+ (1223)336-033; e-mail for inquiry: fileserv@ccdc.cam.ac.uk; e-mail for deposition: deposit@ccdc.cam.ac.uk).

Table 2. Selected Bond Lengths (Å), Bond Angles (°) and Torsion Angles (°) for Complex (**1**)

Fe(1)-O(1)	2.0045(13)	Fe(1)-O(4)	2.0161(13)
Fe(1)-O(2)	2.0149(13)	Fe(1)-N(1)	2.0538(15)
Fe(1)-O(3)	2.0417(13)	Fe(1)-N(2)	2.0552(15)
O(1)-Fe(1)-O(2)	151.86(5)	O(2)-Fe(1)-O(4)	92.07(5)
O(1)-Fe(1)-O(3)	91.06(5)	O(3)-Fe(1)-O(4)	150.97(5)
O(1)-Fe(1)-O(4)	94.25(5)	N(1)-Fe(1)-N(2)	170.90(6)
O(2)-Fe(1)-O(3)	96.57(5)		
O(2)-Fe(1)-O(3)-C(8)	-93.74(13)	O(4)-Fe(1)-O(1)-C(1)	-102.35(14)
O(2)-Fe(1)-O(4)-C(14)	86.75(14)	O(4)-Fe(1)-O(2)-C(7)	94.37(14)

Table 3. Hydrogen Bonds for Complex (**1**)

D-H···A	d(D-H)	d(H···A)	d(D···A)	<DHA
O(1W)-H(1B)···O(6)[#1]	0.85	2.22	3.031(2)	159.3
O(1W)-H(1A)···O(3)[#2]	0.85	2.18	2.976(2)	156.5
O(2W)-H(2B)···O(7)[#2]	0.85	1.93	2.726(2)	155.7
O(2W)-H(2A)···O(3W)[#3]	0.85	1.88	2.732(2)	174.2
O(3W)-H(3A)···O(5)[#4]	0.85	1.90	2.713(2)	160.2
O(3W)-H(3B)···N(3)[#5]	0.85	1.95	2.775(2)	162.1
O(4W)-H(4B)···O(4)	0.85	1.99	2.822(2)	167.5
O(4W)-H(4A)···O(3W)	0.85	1.99	2.838(2)	177.2
N(4)-H(4C)···O(2W)[#6]	0.90	1.82	2.691(2)	163.4

#1: -x+1, -y+1, -z+1; #2: -x, -y+1, -z+1; #3: -x+1, -y, -z+1; #4: x+1, y, z; #5: -x+1, -y+1, -z; #6: x, y+1, z

(Fig. 2) indicates the layered structure for the Fe(III) complex. The space provided between two layers, consisting of (bpyH)$^+$ cations, are filled with a layer of [Fe(pydc)$_2$]$^-$ complex. In fact, the layers involving Fe(III) complex are bridged by (bpyH)$^+$ counter ions *via* hydrogen bondings.

Hydrogen bondings as type O-H···O, O-H···N, and N-H···O between carboxylate, (bpyH)$^+$ and water molecules throughout the lattice of Fe(III) complex play important roles in stabilizing the crystal (Table 3). The C-O···π and C-H···π interactions in this complex were investigated (Fig. 3). The H(17)···Cg1 (Cg1: N(1), C(2)-C(6)) distance is 3.519 Å, the H(5)···Cg2 (Cg2: N(3), C(15)-C(19)) distance is 3.631 Å and the O(8)···Cg3A (Cg3A: N(2A), C(9A)-C(13A)) distance is 3.341 Å [Symmetry code: (A) -x, -y, -z].

X-ray Crystal Structure of [Co$_2$(pydc)$_2$(μ-bpy)(H$_2$O)$_4$].4H$_2$O Complex, (2)

The crystallographic data, selected bond distances, bond angles and intermolecular hydrogen bonds are listed in Tables 1, 4 and 5, respectively. The molecular structure of the complex with atom numbering scheme and the crystal packing diagram are presented in Figs. 4 and 5, respectively. Also, the C-O···π and C-H···π interactions in this complex are shown in Fig. 6.

This complex crystallizes in the space group $P2_1/c$ of the monoclinic system with two molecules per unit cell. The X-ray analysis shows that both pyridine-2,6-dicarboxylate and 4,4´-bipyridine ligands have contributed to the molecular structure. The complex is a binuclear containing two metal fragments, which are linked through 4,4´-bipyridine group. Each Co(II) atom is coordinated by one (pydc)$^{2-}$, one 4,4´-bipyridine and oxygen atoms from two water molecules. Therefore, the Co(II) atom is hexacoordinated *via* two nitrogen atoms N(1), and N(2) and four oxygen atoms O(1), O(4), O(5) and O(6) of carboxylate, 4,4´-bipyridine, and water molecules (Fig. 4). The coordination number will be six for each central atom and the geometry of distorted octahedral is observed around the Co(II) atoms. With respect to the bond angles in the O(5)-Co-O(6) shows deviation from linearity, 176.57(6)° (Table 4).

The non-covalent interactions connect the fragments of the crystal packing (Fig. 5). A wide range of hydrogen bonds (of the type O-H···O) with D···A distances ranging from 2.623(2) to 2.919(3) Å make an extended network based on H-bonding interactions. The non-coordinated water molecules contribute to the formation of this network and increase the number of hydrogen bonds in the structure (Table 5). The strongest hydrogen bonds are between coordinated and uncoordinated water molecules and carboxylate groups. The C-O···π and C-H···π interactions in this complex were investigated (Fig. 6). The O(3)···Cg1 (Cg1: N(1), C(2)-C(6)) and H(4)···Cg2 (Cg2: N(1), C(2)-C(6)) distances are 3.154 and 3.833 Å, respectively. These interactions play important roles in the construction of three dimensional supramolecular network.

253
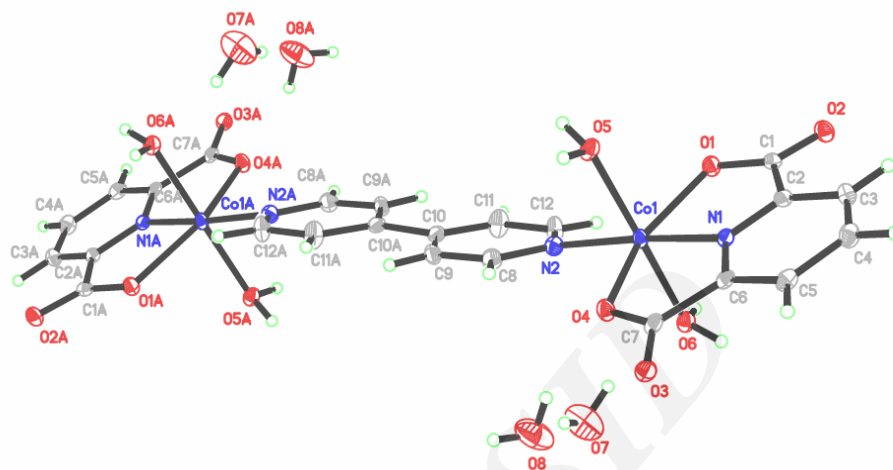
Fig. 4. Molecular structure of the complex (**2**).

Table 4. Selected Bond Lengths (Å), and Bond Angles (°) for Complex (**2**)

Co(1)-O(1)	2.1539(16)	Co(1)-O(6)	2.1217(16)
Co(1)-O(4)	2.1638(16)	Co(1)-N(1)	2.029(2)
Co(1)-O(5)	2.1335(17)	Co(1)-N(2)	2.075(2)
O(1)-Co(1)-O(4)	152.79(6)	N(1)-Co(1)-O(5)	92.75(7)
O(1)-Co(1)-O(5)	88.26(6)	N(1)-Co(1)-O(6)	90.26(7)
O(1)-Co(1)-O(6)	90.81(6)	N(2)-Co(1)-O(1)	108.30(7)
O(4)-Co(1)-O(5)	90.30(6)	N(2)-Co(1)-O(4)	98.77(7)
O(4)-Co(1)-O(6)	92.03(6)	N(2)-Co(1)-O(5)	87.50(7)
O(5)-Co(1)-O(6)	176.57(6)	N(2)-Co(1)-O(6)	89.66(7)
N(1)-Co(1)-O(1)	76.96(7)	N(1)-Co(1)-N(2)	174.73(8)
N(1)-Co(1)-O(4)	75.97(7)		

Table 5. Hydrogen Bonds for Complex (**2**)

D-H···A	d(D-H)	d(H···A)	d(D···A)	<DHA
O(8)-H(8B)···O(4)	0.86	2.03	2.842(3)	156.6
O(8)-H(8A)···O(7)[#1]	0.87	1.93	2.788(4)	168.4
O(5)-H(5A)···O(1)[#2]	0.85	1.93	2.772(2)	168.2
O(5)-H(5B)···O(3)[#1]	0.85	1.88	2.712(2)	167.3
O(6)-H(6B)···O(3)[#3]	0.85	1.91	2.749(2)	169.8
O(6)-H(6A)···O(2)[#4]	0.85	1.77	2.623(2)	175.1
O(7)-H(7A)···O(6)	0.85	2.13	2.919(3)	153.3
O(7)-H(7B)···O(8)	0.85	1.84	2.683(3)	169.6

#1: *x*, -*y*+3/2, *z*-1/2; #2: -*x*+1, -*y*+2, -*z*; #3: *x*, -*y*+3/2, *z*+1/2; #4: -*x*+1, -*y*+2, -*z*+1.

254
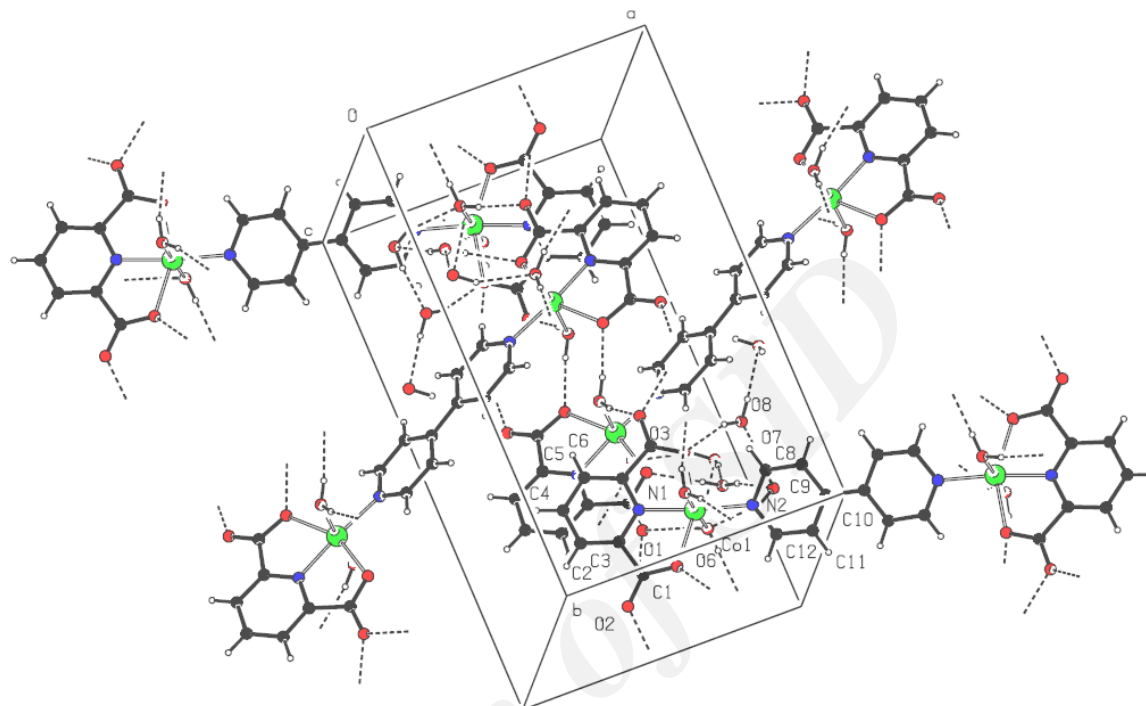
Fig. 5. Crystal packing diagram of complex (**2**).
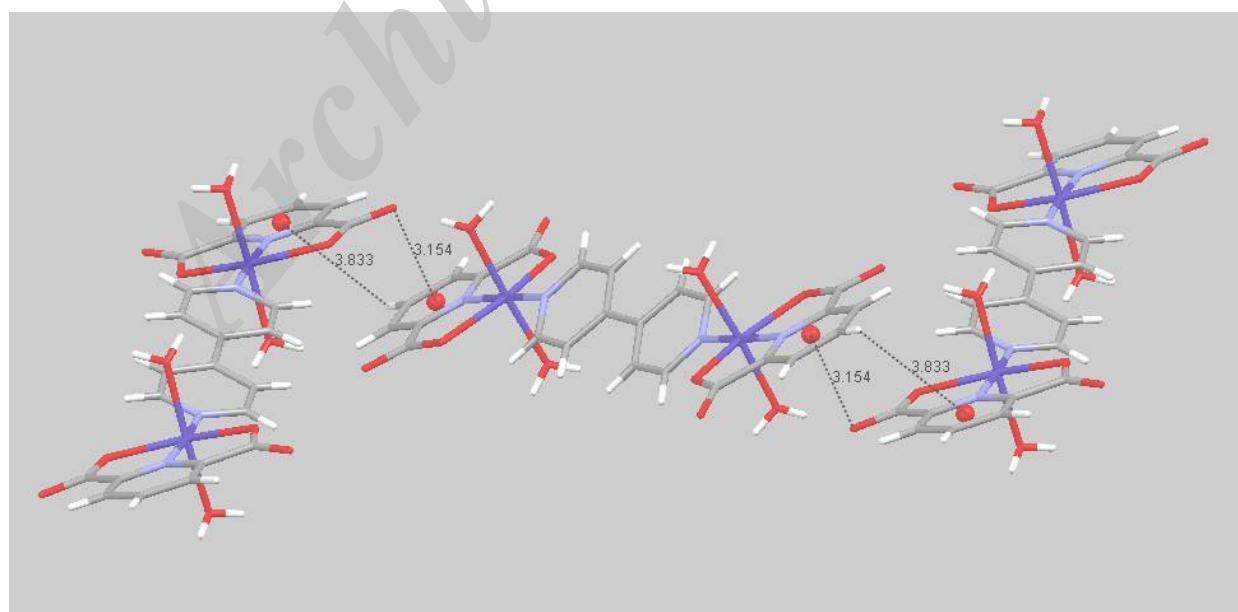
Fig. 6. The C-O···π and C-H···π interactions in complex (**2**).

X-ray Crystal Structure of [Ni(pydc)(bpy)(μ-bpy)]₄. 8H₂O Complex, (3)

The molecular structure and the crystal packing diagram of complex (**3**) are shown in Figs. 7 and 8, respectively. Table 1 lists a summary of X-ray crystallographic data and Table 6 shows selected bond lengths, and angles for this complex. A list of hydrogen bonds is also given in Table 7.

This complex crystallizes in the space group $P2_1/c$ of the monoclinic system with two molecules per unit cell. The molecular structure of this complex is built of tetranuclear units of $[Ni(pydc)(bpy)(\mu\text{-bpy})]_4$, in which each $(pydc)^{2-}$ moiety has acted as a tridentate ligand. The 4,4´-bipyridine, which was present in the reaction mixture involved in the resulting Ni(II) complex. Each Ni(II) atom is coordinated by one unit of pyridine-2,6-dicarboxylate and three units of 4,4´-bipyridine (Fig. 7). The geometry of the nickel(II) atom is distorted octahedral, in which the N(6)-Ni(1)-N(8) angle shows deviation from linearity, 178.70(12)° (Table 6).

The hydrogen bonding existing in the Ni(II) complex is as types O-H···O, and O-H···N with D···A distances ranging from 2.516(11) to 3.231(7) Å make an extended network based on H-bonding interactions. Investigation of the packing diagram confirms that the structure is stabilized by hydrogen bonds (Fig. 8).

Solution Studies

In preliminary experiments, the fully protonated forms of pydc (L) and bpy (Q) were titrated with a standard NaOH solution in order to obtain some information about their protonation constants as the building blocks of the pydc-bpy adduct. The protonation constants of pydc [15,22] and bpy were calculated by fitting the volume-*p*H data to the BEST program. The results are summarized in Table 8. It is noteworthy that the resulting logβ values are in satisfactory agreement with those reported for family of bpy [26] in the literature. The evaluation of the equilibrium constants for the reactions of pydc with bpy in different protonation forms was accomplished through comparison of the calculated and
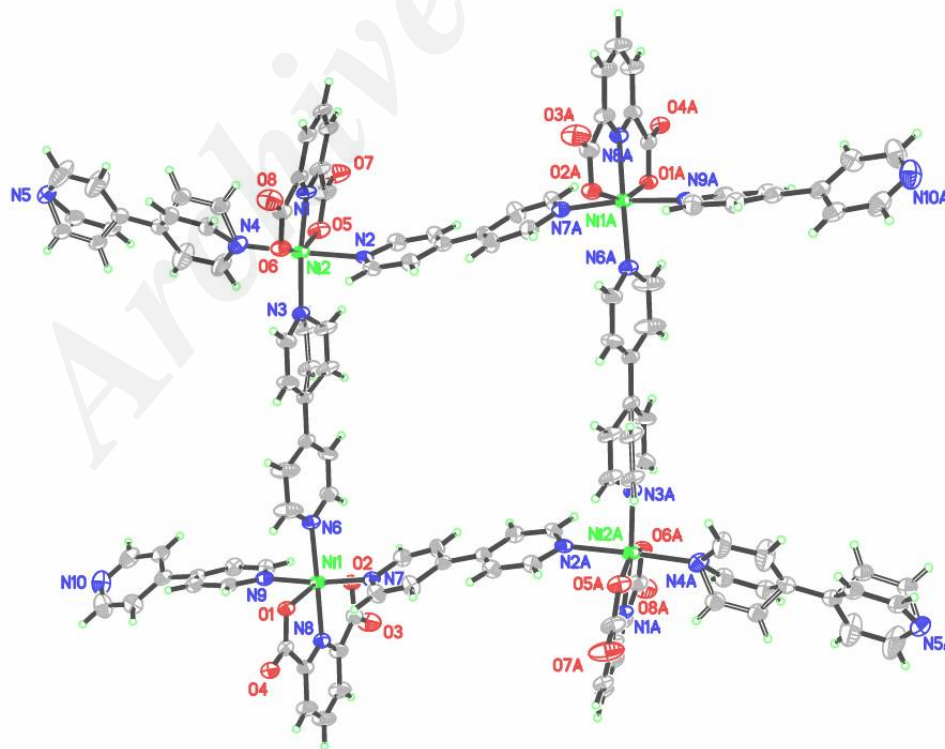

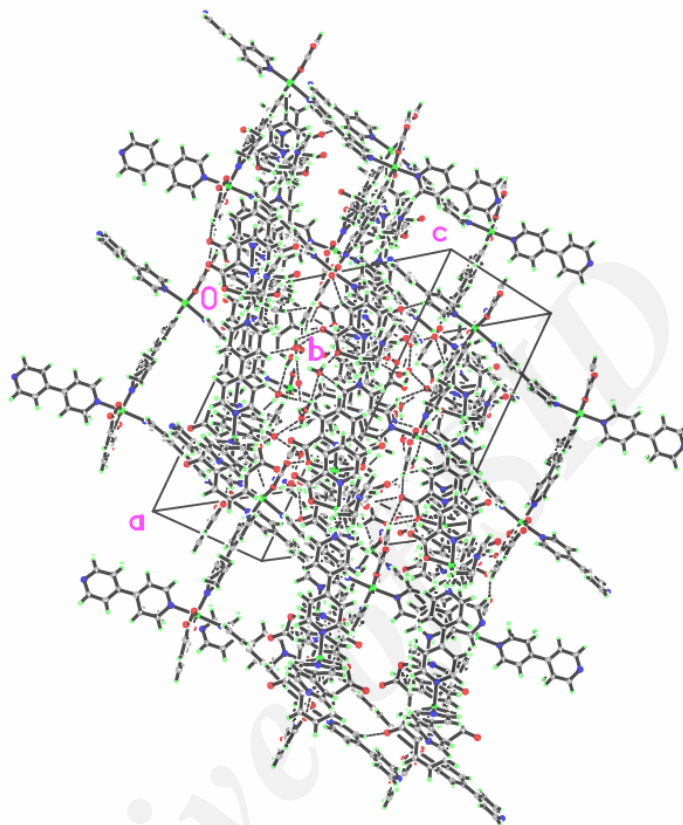**Fig. 7.** Molecular structure of complex (**3**).

Fig. 8. Crystal packing diagram of complex (**3**).

Table 6. Selected Bond Lengths (Å) and Bond Angles (°) for Complex (**3**)

Ni(1)-O(1)	2.088(2)	Ni(2)-O(5)	2.124(3)
Ni(1)-O(2)	2.125(2)	Ni(2)-O(6)	2.110(2)
Ni(1)-N(6)	2.056(3)	Ni(2)-N(1)	1.973(3)
Ni(1)-N(7)	2.148(3)	Ni(2)-N(2)	2.170(3)
Ni(1)-N(8)	1.982(3)	Ni(2)-N(3)	2.025(3)
Ni(1)-N(9)	2.124(3)	Ni(2)-N(4)	2.146(3)
O(1)-Ni(1)-O(2)	156.00(9)	O(5)-Ni(2)-O(6)	156.45(9)
O(1)-Ni(1)-N(6)	100.98(10)	O(5)-Ni(2)-N(1)	77.94(11)
O(1)-Ni(1)-N(7)	89.62(10)	O(5)-Ni(2)-N(2)	91.78(11)
O(1)-Ni(1)-N(8)	77.83(10)	O(5)-Ni(2)-N(3)	100.43(11)
O(1)-Ni(1)-N(9)	92.35(11)	O(5)-Ni(2)-N(4)	89.54(11)
O(2)-Ni(1)-N(6)	102.95(11)	O(6)-Ni(2)-N(1)	78.65(11)
O(2)-Ni(1)-N(7)	90.34(10)	O(6)-Ni(2)-N(2)	89.04(11)
O(2)-Ni(1)-N(8)	78.26(10)	O(6)-Ni(2)-N(3)	103.12(11)
O(2)-Ni(1)-N(9)	90.47(11)	O(6)-Ni(2)-N(4)	88.60(11)
N(6)-Ni(1)-N(7)	85.64(11)	N(1)-Ni(2)-N(2)	85.60(11)
N(6)-Ni(1)-N(8)	178.70(12)	N(1)-Ni(2)-N(3)	174.13(12)
N(6)-Ni(1)-N(9)	87.68(11)	N(1)-Ni(2)-N(4)	91.83(12)
N(7)-Ni(1)-N(8)	94.82(11)	N(2)-Ni(2)-N(3)	88.83(11)
N(7)-Ni(1)-N(9)	173.29(11)	N(2)-Ni(2)-N(4)	176.81(11)
N(8)-Ni(1)-N(9)	91.86(11)	N(3)-Ni(2)-N(4)	93.80(12)

257

Table 7. Hydrogen Bonds for Complex (**3**)

D-H···A	d(D-H)	d(H···A)	d(D···A)	<DHA
O(1W)-H(1A)···O(2W)	0.87	2.05	2.795(10)	144.1
O(1W)-H(1B)···O(4W)[#1]	0.84	2.31	3.095(11)	156.8
O(2W)-H(2B)···O(5)	0.85	1.96	2.798(4)	169.2
O(2W)-H(2A)···N(5)[#2]	0.85	2.01	2.785(5)	151.3
O(4W)-H(4A)···O(1W)[#1]	0.85	2.38	3.095(11)	142.7
O(4W)-H(4B)···O(3WB)	0.85	1.66	2.516(11)	178.9
O(4W)-H(4B)···O(3WA)	0.85	2.09	2.912(8)	161.4
O(5W)-H(5A)···O(8W)	0.85	2.04	2.887(7)	179.5
O(5W)-H(5B)···O(7)[#3]	0.85	2.41	2.880(6)	115.3
O(6W)-H(6B)···O(4)[#4]	0.85	1.96	2.765(4)	158.1
O(6W)-H(6A)···O(2)[#5]	0.85	2.01	2.845(4)	168.2
O(6W)-H(6A)···O(3)[#5]	0.85	2.54	3.176(4)	132.9
O(7W)-H(7B)···O(5W)[#6]	0.85	2.07	2.693(7)	129.5
O(7W)-H(7A)···O(1W)[#7]	0.85	2.08	2.551(12)	114.2
O(7W)-H(7A)···O(2W)[#7]	0.85	2.41	3.231(7)	162.1

#1: -x+1, -y+1, -z+1; #2: x, -y+1/2, z+1/2; #3: x, y, z-1; #4: x+1, y-1, z; #5: -x+1, y-1/2, -z+3/2;#6: x, -y+3/2, z+1/2; #7: -x+1, y+1/2, -z+3/2.

Table 8. Overall Stability and Stepwise Protonation Constants of pydc and bpy and Recognition Constants for Interaction between them in Aqueous Solution at 25 °C and μ = 0.1 M KNO$_3$

| Stoichiometry							
bpy	pydc	h	logβ	Equilibrium quotient K	logK	Max%	*p*H
0	1	1	5.20	-	5.20	89.5	4.0
0	1	2	7.92	-	2.72	84.2	2.0
1	0	1	5.24	-	5.24	83.5	4.2
1	0	2	8.47	-	3.23	94.3	2.0
1	1	1	9.17	[bpypydcH]/[bpyH][pydc]	3.93	96.2	6.4
1	1	2	13.59	[bpypydcH$_2$]/[bpyH][pydcH]	3.15	55.8	4.0
1	1	3	17.18	[bpypydcH$_3$]/[bpyH][pydcH$_2$]	4.02	94.7	2.0
				[bpypydcH$_3$]/[bpyH$_2$][pydcH]	3.51		

experimental pH profiles, obtained with both pydc and bpy present [15,24,27]. Distribution diagrams for bpy are shown in Fig. 9c and all evaluated overall stability and stepwise protonation constants are given in Table 8. The corresponding species distribution diagram for pydc-bpy is shown in Fig. 10. As it is obvious, the most abundant adduct species between pydc and bpy, present at pH values of 6.4 (96.2%), 4.0 (55.8%) and 2.0 (94.7%) are bpy-pydcH (logK = 3.93), bpyH-pydcH (logK = 3.15) and bpyH-pydcH$_2$ (logK = 3.51).

In order to evaluate the stoichiometry and stability of Fe^{3+}, Co^{2+} and Ni^{2+} complexes with pydc-bpy adduct in aqueous solution, the equilibrium potentiometric pH titration profiles of pydc [22,28], bpy and their 1:1 mixture were obtained in the absence and presence of the Fe^{3+}, Co^{2+} and Ni^{2+} ions. The resulting pH profiles are shown in Figs. 9a, 9b and 13a. In all cases, the titration of ligands in the presence of metal ions was stopped when the precipitate formation observed. Figure 9a and 13a clearly indicate the titration curves of both that the potentiometric titration curves for pydc and pydc-bpy in the presence of all three metal ions studies are depressed considerably. While, Fig. 9b shows that, in contrast to Fe^{3+}, the Ni^{2+} and Co^{2+} ions possess very weak interactions with bpy, as is clear from negligible depression of the corresponding titration curves.

As mentioned in our previous publications [15,22], the cumulative stability constants for the resulting M$_m$L$_l$Q$_q$H$_h$ complexes is defined as β_{mlqh}, where M, L, Q and H denote the metal ion, pydc, bpy and proton, respectively, and m, l, q, and h are the respective stoichiometric coefficients. The cumulative stability constants for all complexes formed in aqueous solution were evaluated by fitting the corresponding pH titration curves to the BEST program [25], and the resulting values for the most likely complexed species in are also included in Table 9. All the corresponding distribution diagrams are also shown in Figs. 11-13. The results thus obtained clearly revealed that, with the exception of Ni^{2+} and Co^{2+} ions that form relatively weak complexes with bpy, all the three metal ions form stable complexes with bpy, pydc and pydc-bpy systems in solution.

As it is obvious from Fig. 11 and Table 9, in the case of pydc (L) as ligand, the most likely species for Co^{2+} are CoL, CoLH$_2$, CoL$_2$ and CoL$_2$H. Such complexed species for Fe^{3+}-pydc and Ni^{2+}-pydc systems are reported in our previous
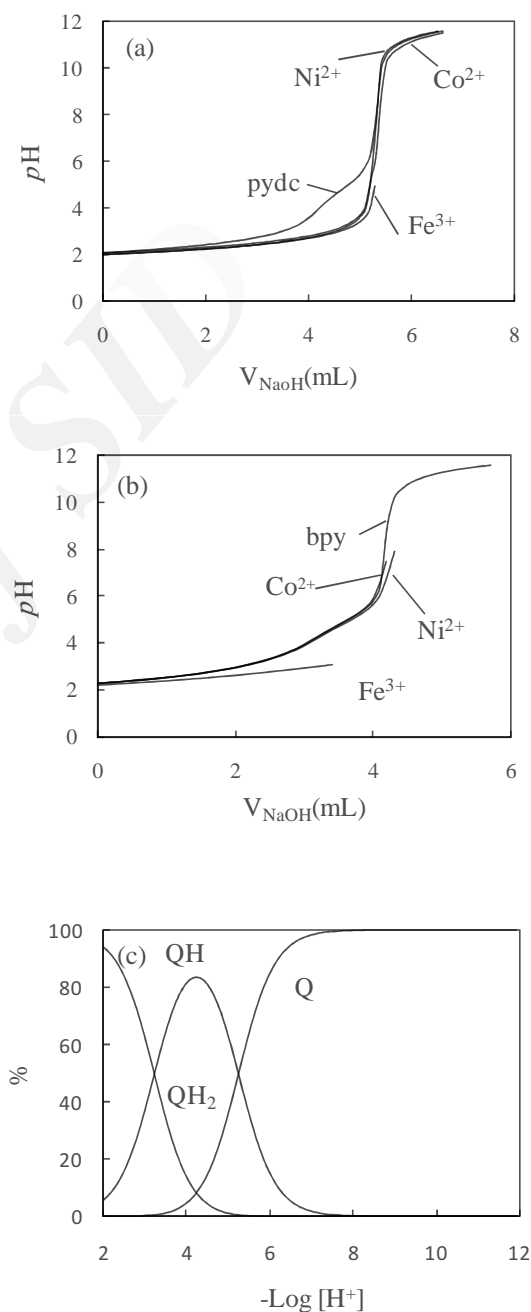
Fig. 9. Potentiometric titration curves of pydc (a) and bpy (b) in the absence and presence of M^{n+} ions with NaOH 0.0927 M in aqueous solution at 25 °C and μ = 0.1 M KNO$_3$ M = Fe^{3+}, Co^{2+} and Ni^{2+} and distribution diagrams of bpy(Q) (c).

259
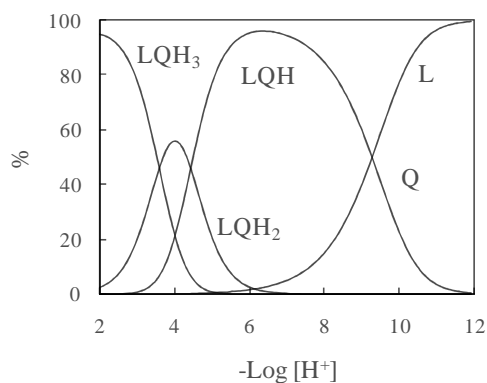
Fig. 10. Distribution diagram of hydrogen bonding interaction between the various protonated forms of bpy(Q) and pydc(L).

papers [22,28].

Figure 12 and Table 9 show that for the bpy-M system, the most likely species for Fe^{3+} are FeQ_2, Fe_2Q_2H, $FeQ_2H_{(-2)}$ and Fe_2Q_2, and for Co^{2+} are Co_2Q and CoQ_2 and for Ni^{2+} are NiQ, Ni_2Q and Ni_2Q_2.

Figures 13b-d and Table 9, revealed the formation of a variety of ternary complexes between the above-mentioned cations and the pydc-bpy adduct system at different ranges of *p*H. The predominant species for Fe^{3+} are: $FeLQ_2H$ (at *p*H 2.1), FeL_2QH (at *p*H 3.4-4.0), FeL_2QH_2 (at *p*H 2.0), FeL_2Q_2 (at *p*H 5.7) and $FeL_2Q_2H_2$ (at *p*H 3.6), for Ni^{2+} are: NiL_2QH_2 (at *p*H 2.0), $NiLQ_2$ (at *p*H > 10.6), $NiLQ_2H$ (at *p*H 3.2), NiL_2QH (at *p*H 5.7), and $NiLQ_2H_3$ (at *p*H 2.0) and for Co^{2+} are: Co_2L_2Q (at *p*H 2.0), CoL_2Q (at *p*H < 8.3), CoL_2QH (at *p*H 4.5) and

Table 9. Overall Stability Constants of bpy/pydc/M^{n+}(q/l/m) Binary and Ternary Systems in Aqueous Solution at 25 °C and $\mu = 0.1$ M KNO_3 (M^{n+} = Fe(III), Co(II), Ni(II))

System	m	l	q	h	logβ	Max%	at *p*H
	1	0	2	0	12.02	90.4	3.0
	1	0	1	0	5.94	Negligible	-
	1	0	1	1	8.58	Negligible	-
	2	0	1	0	8.69	Negligible	-
Fe-bpy	2	0	2	1	17.52	29.2	2.0
	1	0	1	-1	2.30	Negligible	-
	1	0	1	-2	-0.85	Negligible	-
	1	0	2	-1	5.28	Negligible	-
	1	0	2	-2	4.53	2.8	3.0
	2	0	2	0	14.77	5.6	2.1
	1	1	0	0	6.32	2.4	2.1-2.4
Co-pydc	1	1	0	2	10.93	9.0	2.0
	1	2	0	0	12.10	99.8	>5.8
	1	2	0	1	14.66	69.4	2.0
Co-bpy	2	0	1	0	1.46	28.0	3.9
	1	0	2	0	1.79	79.0	7.4
	1	0	1	0	2.23	42.8	>6.5
Ni-bpy	2	0	1	0	3.84	40.2	3.0
	2	0	2	0	4.47	24.0	>6.6

260

Table 9. Continued

|							
	1	1	2	1	25.95	5.2	2.1
	1	1	1	0	13.63	Negligible	-
	1	1	1	1	20.73	Negligible	-
	1	2	2	1	27.23	Negligible	-
Fe-pydc-bpy	1	2	1	0	23.59	Negligible	-
	1	2	1	1	28.17	3.2	3.4-4.0
	1	2	1	2	31.55	44	2.0
	1	2	2	0	26.98	96.4	5.7
	1	2	2	2	36.36	91.6	3.6
	1	2	1	0	19.05	99.8	8.3<
	1	2	1	1	23.99	73	4.5
Co-pydc-bpy	1	2	1	2	24.28	89	2.0
	2	1	1	0	23.46	Negligible	-
	2	2	1	0	29.94	4.4	2.0
	1	1	2	0	19.76	99.6	10.6<
	1	1	2	1	23.96	38.2	3.2
	1	1	2	3	27.66	6.8	2.0
	1	1	1	0	11.96	Negligible	-
Ni-pydc-bpy	1	1	1	1	18.37	Negligible	-
	1	2	1	0	14.26	Negligible	-
	1	2	1	1	25.23	48.8	5.7
	1	2	1	2	29.16	76.4	2.0
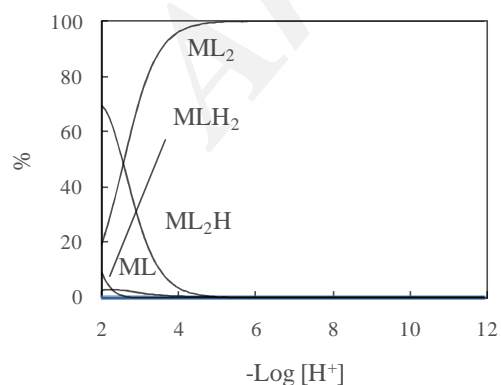
Fig. 11. Distribution diagrams of pydc(L)/M binary systems, $M = Co^{2+}$.

CoL_2QH_2 (at pH 2.0). It is interesting to note that the stoichiometries of some of the most abundant ternary complexes, existing in aqueous solution, are very similar to those reported for the corresponding isolated complexes in the solid state.

CONCLUSIONS

We have investigated that the reaction between metal ions with pyridine-2,6-dicarboxylic acid and 4,4′-bipyridine adduct leads to the formation of various complexes. The intermolecular forces consisting of H-bonding, ion-pairing and π-interactions, play important roles in the construction of extended networks in the crystal systems. The solution

261
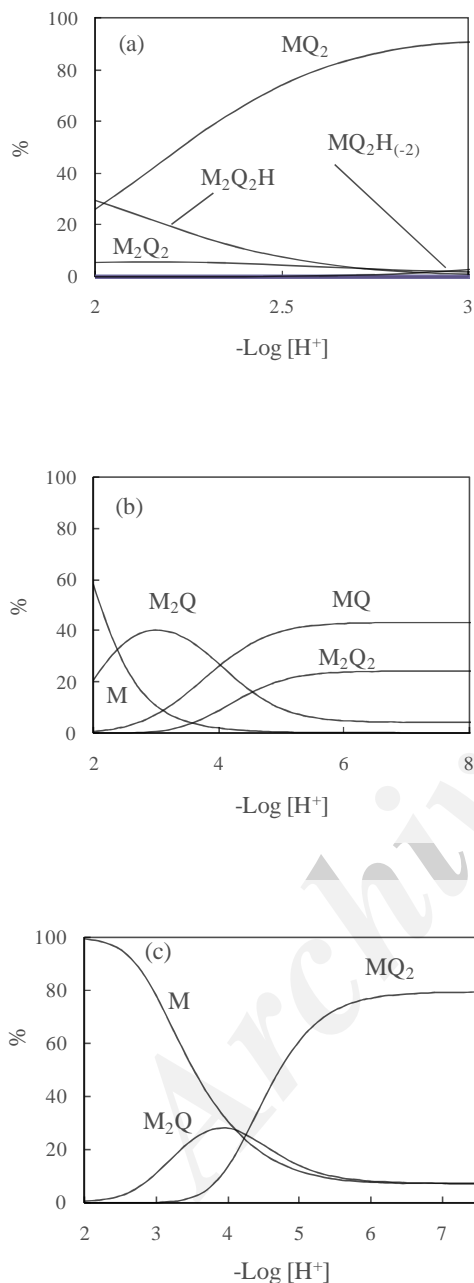
Fig. 12. Distribution diagrams of bpy(Q)/M binary systems, M = Fe^{3+} (a), Ni^{2+} (b) and Co^{2+} (c).

potentiometric studies provided additional evidences of the interaction between adduct with metal ions, supporting the results obtained from the solid state studies.
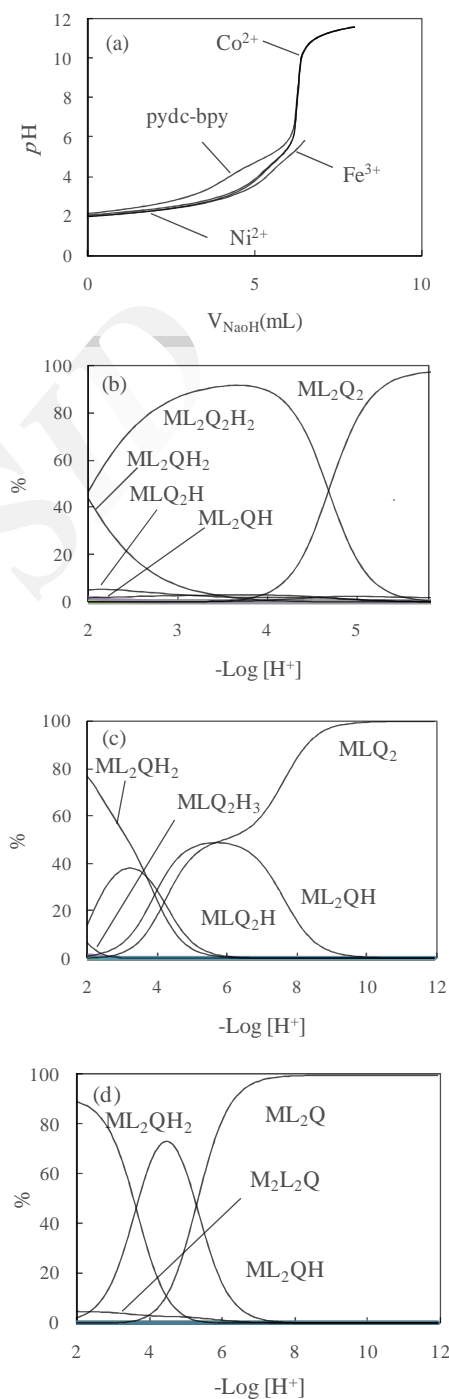
Fig. 13. Potentiometric titration curves of pydc+bpy in the absence and presence of M^{n+} ions with NaOH 0.0927 M in aqueos solution at 25 °C and μ = 0.1 M KNO_3, M = Fe^{3+}, Co^{2+} and Ni^{2+} (a) and distribution diagrams of pydc(L)/bpy(Q)/M ternary systems, M = Fe^{3+} (b), Ni^{2+} (c) and Co^{2+} (d).

ACKNOWLEDGMENTS

REFERENCES

[1] a) A.N. Khlobystov, A.J. Blake, N.R. Champness, D.A. Lemenovskii, A.G. Majouga, N.V. Zyk, M. Schröder, Coord. Chem. Rev. 222 (2001) 155; b) S.A. Barnett, A.J. Blake, N.R. Champness, J.E.B. Nicolson, C.L. Wilson, J. Chem. Soc. Dalton Trans. (2001) 567; c) L. Carlucci, G. Ciani, D.M. Proserpio, S. Rizzato, J. Chem. Soc. Chem. Commun. (2001) 1198; d) D.-L. Long, A.J. Blake, N.R. Champness, M. Schröder, J. Chem. Soc. Chem. Commun. (2000) 2273; e) L. Carlucci, G. Ciani, D.M. Proserpio, S. Rizzato, J. Chem. Soc. Dalton Trans. (2000) 3821; f) D.-L. Long, A.J. Blake, N.R. Champness, M. Schröder, J. Chem. Soc. Chem. Commun. (2000) 1369; g) R. Robson, J. Chem. Soc. Dalton Trans. (2000) 3735.

[2] a) S.A. Bourne, J. Lu, B. Moulton, M.J. Zaworotko, J. Chem. Soc. Chem. Commun. (2001) 861; b) A.J. Blake, P. Hubberstey, U. Suksangpanya, C.L. Wilson, J. Chem. Soc. Dalton Trans. (2000) 3873; c) G.R. Desiraju, J. Chem. Soc. Dalton Trans. (2000) 3745; d) M. Munakata, L.P. Wu, M. Yamamoto, T. Kuroda-Sowa, M. Maekawa, J. Am. Chem. Soc. 118 (1996) 3117; e) M.M. Chowdhry, D.M.P. Mingos, A.J.P. White, D.J. Williams, J. Chem. Soc. Chem. Commun. (1996) 899; f) C.B. Aakeröy, A.M. Beatty, K.R. Lorimer, J. Chem. Soc. Dalton Trans. (2000) 3869.

[3] J.A. Swift, A.M. Pivovar, A.M. Reynolds, M.D. Ward, J. Am. Chem. Soc. 120 (1998) 5887.

[4] M.C. Etter, Acc. Chem. Res. 23 (1990) 120.

[5] a) G. Smith, U.D. Wermuth, J.M. White, Aust. J. Chem. 54 (2001) 171; b) G. Smith, U.D. Wermuth, R.C. Bott, J.M. White, A.C. Willis, Aust. J. Chem. 54 (2001) 165; c) G. Smith, R.C. Bott, A.D. Rae, A.C. Willis, Aust. J. Chem. 53 (2000) 531; d) G. Smith, C.E. Pascoe, C.H.L. Kennard, K.A. Byriel, Aust. J. Chem. 52 (1999) 71; e) D.E. Lynch, G. Smith, K.A. Byriel, C.H.L. Kennard, Aust. J. Chem. 47 (1994) 1789; f) D.E. Lynch, G. Smith, K.A. Byriel, C.H.L. Kennard, A.K. Whittaker, Aust. J. Chem. 47 (1994) 309.

[6] A. Moghimi, M. Ranjbar, H. Aghabozorg, F. Jalali, M. Shamsipur, G.P.A. Yap, H. Rahbarnoohi, J. Mol. Struct. 605 (2002) 133.

[7] A. Moghimi, M. Ranjbar, H. Aghabozorg, F. Jalali, M. Shamsipur, R.K. Chadha, J. Chem. Res. (2002) 1047.

[8] M. Ranjbar, M. Taghavipur, H. Aghabozorg, A. Moghimi, F. Jalali, M. Shamsipur, Pol. J. Chem. 76 (2002) 785.

[9] A. Moghimi, M. Ranjbar, H. Aghabozorg, F. Jalali, M. Shamsipur, R.K. Chadha, Can. J. Chem. 80 (2002) 1687.

[10] A. Moghimi, A. Shokrollahi, M. Shamsipur, H. Aghabozorg, M. Ranjbar, J. Mol. Struct. 701 (2004) 49.

[11] A. Moghimi, R. Alizadeh, A. Shokrollahi, H. Aghabozorg, M. Shamsipur, A. Shockravi, Inorg. Chem. 42 (2003) 1616.

[12] H. Aghabozorg, F. Manteghi, S. Sheshmani, J. Iran. Chem. Soc. 5 (2008) 184.

[13] S. Sheshmani, H. Aghabozorg, F. Mohammad Panah, R. Alizadeh, G. Kickelbick, B. Nakhjavan, A. Moghimi. F. Ramezanipour, H.R. Aghabozorg, Z. Anorg. Allg. Chem. 632 (2006) 469.

[14] A. Moghimi, V. Lippolis, H. Aghabozorg, A. Shokrollahi, M. Shamsipur, S. Sheshmani, A.J. Blake, Polish J. Chem. 80 (2006) 1385.

[15] A. Moghimi, S. Sheshmani, A. Shokrollahi, M. Shamsipur, G. Kickelbick, H. Aghabozorg, Z. Anorg. Allg. Chem. 631 (2005) 160.

[16] J. Soleimannejad, H. Aghabozorg, S. Hooshmand, M. Ghanbari, F. Manteghi, M. Shamsipur, J. Iran. Chem. Soc. 7 (2010) 405.

[17] S. Sheshmani, P. Dalir Kheirollahi, H. Aghabozorg, A. Shokrollahi, G. Kickelbick, M. Shamsipur, F. Ramezanipour, A. Moghimi, Z. Anorg. Allg. Chem. 631 (2005) 3058.

[18] F. Ramezanipour, H. Aghabozorg, A. Shokrollahi, M. Shamsipur, H. Stoeckli-Evans, J. Soleimannejad, S. Sheshmani, J. Mol. Struct. 779 (2005) 77.

[19] A. Moghimi, S. Sheshmani, A. Shokrollahi, H. Aghabozorg, M. Shamsipur, G. Kickelbick, M.C. Aragoni, V. Lippolis, Z. Anorg. Allg. Chem. 630

263

(2004) 617.

[20] G.M. Sheldrick, SADABS. University of Göttingen, Germany, 1996.

[21] G.M. Sheldrick, SHELXS97 and SHELXL97. University of Göttingen, Germany, 1997.

[22] H. Aghabozorg, F. Ramezanipour, J. Soleimannejad, M.A. Sharif, A. Shokrollahi, M. Shamsipur, A. Moghimi, J. Attar Gharamaleki, V. Lippolis, A.J. Blake, Polish J. Chem. 82 (2008) 487.

[23] A. Shokrollahi, M. Ghaedi, H.R. Rajabi, M.S. Niband, Spectrochim. Acta Part A. 71 (2008) 655.

[24] H. Aghabozorg, F. Manteghi, M. Ghadermazi, M. Mirzaei, A.R. Salimi, A. Shokrollahi, S. Derki, H. Eshtiagh-Hosseini, J. Mol. Struct. 919 (2009) 381.

[25] A.E. Martell, R.J. Motekaitis, Determination and Use of Stability Constants, 2nd ed., VCH, New York, 1992.

[26] M. Irimia, G. Lisa, R. Danac, N. Aelenei, I. Druta Croat, Chem. Acta 77 (2004) 587.

[27] J.B. English, A.E. Martell, R.J. Motekaitis, I. Murase, Inorg. Chim. Acta 258 (1997) 183.

[28] H. Aghabozorg, E. Sadr-khanlou, A. Shokrollahi, M. Ghaedi, M. Shamsipur, J. Iran. Chem. Soc. 6 (2009) 55.